Fast Fourier transform for fingerprint enhancement and features extraction with adaptive block size using orientation fields

AIT AOUDIA Amina[1,*] *MICHELUCCI Dominique*[2] *ZAFOUNE Youcef*[1]

[1]*Université des Sciences et de la Technologie Houari Boumediene (USTHB), BP 32 Bab Ezzouar, 16111 - Alger, Algeria*
[2]*Laboratoire d'Informatique de Bourgogne (LIB), EA 7534, 21000 Dijon, France*
[*]*Corresponding author. Email: aaitaoudia@usthb.dz*

ABSTRACT
Extracting minutiae from a digital fingerprint is a crucial step in a fingerprint-based recognition systems. This work deals with poor-quality fingerprint images containing broken ridges. The enhancement stage connects broken ridges and is essential for extracting correct minutiae. We use a FFT variant [8] for this stage, but, to truly benefit from FFT in a block, it is essential to determine a suitable block size, depending on ridges orientation field. We propose to use a quadtree to partition the ridges orientation field into homogeneous blocks. A block is homogeneous when at least seventy percent of its ridges orientations are within ten degrees. Another issue addressed in this article is the choice of a suitable neighborhood window size W for computing orientation field image, depending on the fingerprint image quality. The performance improvements of our algorithm are evaluated and compared with standard measures MSE, PSNR and GI, on databases DB1 to DB4 of FVC2004 and NIST special database SD302d.

Keywords: *Minutiae, fingerprint enhancement, orientation field, quadtree decomposition, FFT.*

1 Introduction

Fingerprints are unique to each person and each finger has its own unique fingerprint. The probability for two people to share the same fingerprints is infinitesimal. Fingerprints recognition and verification tend to become the most used in biometric systems, and is one of the challenging Pattern Recognition problems.

Fingerprint recognition is generally composed of four stages. The first stage is the acquisition of the fingerprint grayscale image.

The second is the pre-processing that includes enhancement, binarization and thinning of the fingerprint. The enhancement is used for two main reasons: 1- to connect broken ridges of fingerprint, and 2- to eliminate noise between ridges [1].

The third stage extracts features from the thinned image. In most of fingerprint recognition systems, this stage is based on minutiae features [2]. There are two types of minutiae: starting or ending points of a ridge, and bifurcation points shared by three incident ridges (Figure 1).

Figure 1: Fingerprint image

A minimum number of matching pairs of minutiae is required to declare that two fingerprints are from the same person. Some countries legally require at least 12 minutiae matches. Other countries such as Italy even have higher standards and require 16 to 17 minutiae matches [13].

The fourth stage matches minutiae for identification and verification.

In an ideal acquisition of a fingerprint, it is easy to detect minutiae by following the detected ridge lines to their ending and bifurcation points. But, in practice, the fingerprint can be corrupted and several relevant information may not appear due to multiple reasons, like the non-cooperative behaviour of the individual when harvest the sample, the poor performance of the scanning device, or user' dry hands [4]. Fingerprint image enhancement is an essential preprocessing stage for avoiding the feature extraction stage to detect wrong minutiae features, therefore this stage is critical for fingerprint recognition systems, and especially for reducing false rejection rates [3].

AFIS (Automatic Fingerprint Identification Systems) perform most operations: segmentation and estimation of orientation field, at block level. Thus, it is important to choose a suitable block size for optimal extraction of features in fingerprint images. A too large block size tends to generate misinformation and to increase the number of information irrelevant for the pattern, while a too small block size causes failures in connecting broken ridges for fingerprint images with poor quality. Several approaches [5, 6, 7] have been proposed in the literature to choose a suitable block size. In many articles including [5, 6, 7], the ridges orientation field is partitioned into blocks with an initial block size (with article-dependent value), then some homogeneity criteria is evaluated: if the block is not homogeneous enough, then the local orientation field in this region is re-computed at a lower resolution, with a smaller block size until the consistency level fulfils the criteria. The homogeneity criterium is article-dependent. The initial block sizes and thresholds are determined empirically by trial and errors, depending on fingerprint images. In [5, 6], the block size is the same for the whole image. In [9], the block size depends on the inter-ridge distance, which is non constant in the fingerprint.

Shalash et al. [6] present a simple and fast modification for enhancement, based on the usage of Gabor filters technique. The ridge frequency of fingerprint images is quickly estimated and then used to choose the block size for computing the block orientation field of the current region of the fingerprint. This block size is also used as an input parameter for the Gabor filter: the latter inputs a frequency bandwidth and the orientation field.

Tahmasebi et al. [7] estimate the ridge frequency for each block of the image. In order to reduce the computational cost, the average ridge distance is computed once for the whole input image with a constant initial block size. For each region, in order to compute a correct average inter-ridge distance value, a search is done on all directions and blocks of the region, to find the block and the direction with the least variance in direction, which determines a clear foreground area. Based on the corresponding blocks, an averaging summation of directions is performed along the ridge-dominant direction, to find ridge starting and ending points. The mean of the obtained inter-ridge distances is then assigned as the average ridge distance of the image. For each block of the region, its (at most nine) adjacent blocks in the region are selected for the next stage: the average inter-ridge distance of the image is the main parameter used to determine the block size and the filter mask size, valid for all the image. Knowing the size of the mask, other proposed filter parameters can be determined. The image is then enhanced using the directional filtering method.

We propose an algorithm which decomposes the image fingerprint according to its orientation field, using a quadtree. The main idea is to split the studied block until some orientation homogeneity threshold is reached: we consider that a block is homogeneous when at least seventy percent of its ridges orientation values are within ten degrees. An advantage of our approach is that few parameters are needed to compute the best decomposition block size.

The image enhancement algorithm is mainly aimed at connecting broken edges, removing noise between ridges and enhancing the contrast of ridges and valleys. Histogram equalization, FFT-based transform, and Gabor filter-based methods are the three ways for image enhancement. It has been found that Gabor filter-based method is computationally expensive [1].

We use a variant of Fast Fourier Transform (as [8]) to enhance generated blocks of the fingerprint image. Our algorithm connects more broken ridges (Fig. 7) and achieves a better goodness index (Tab. 6) than previous ones.

Plane. Section 2 describes steps of the proposed algorithm, Section 3 the computation of the orientation field, Section 4 the decomposition into homogeneous blocks, Section 5 the features extraction and post-processing, Section 6 implementations, results and comparisons. Section 7 concludes.

2 The proposed algorithm

Following Neethu et al. [8], we enhance fingerprint using $FFT \times \mid FFT \mid^k$ filter. FFT on a block allows reconnection of broken ridges. In [8], the image decomposition is done by choosing an apriori block size. However, reconnection fails when a too small block size is chosen to enhance a fingerprint image of bad quality. In our approach, a suitable block size is chosen by the algorithm, according to the ridge orientation field. We use a quadtree to recursively subdivide the orientation field of the fingerprint: its leaves represent homogeneous blocks. A block is homegeneous when at least seventy percent of its ridge orientations are within a ten degrees angle. The different steps of our method are given below.

1- The fingerprint image is cropped so that its width and height are multiple of W. Then histogram equalization is performed.

2- The orientation field is estimated, on the whole image, using a gradient-based method [9]. The main steps of process are shown in section 3.

3. The fingerprint image is recursively decomposed into homogeneous blocks, using a quadtree. See section 4. Each homogeneous block corresponds to a quadtree leave and is suitable for enhancement.

4- Fast Fourier Transform of each homogeneous block is computed. The magnitude of the FFT is taken and raised to some real value k. This is then multiplied by the original FFT. To compute the new enhanced block in the frequency domain, the inverse Fourier transform is then computed as follows (1):

$$P(x,y) = FFT^{(-1)}[FFT(I(x,y)) \times \mid FFT(I(x,y)) \mid^k] \quad (1)$$

where $I(x,y)$ is the grayscale value in the fingerprint block and $P(x,y)$ the grayscale value in the enhanced block. k is an experimentally determined constant. We tried several values for k between 0.45 and 0.70, and finally chose $k = 0.45$ as [16]. Figure 3 shows that this FFT variant gives more accurate results than the standard FFT (with $k = 1$), and the stability of thinning and enhancement results for $k \in [0.45, 0.55]$. After performing the FFT, the following steps are carried out on the current block:

- smoothening using a Gaussian filter.
- adjusting contrast using a Butterworth filter.

5- Binarizing the whole enhanced image P. According to [10], adaptive thresholding technique is better than global thresholding. An adaptive thresholding is used to binarize the enhanced image P [11]. We compute a locally adaptive threshold for binarization. The choice of the threshold is based on the local mean intensity (first-order statistics) in the neighborhood of each pixel. In our case, the neighborhood size used to compute local statistic around each pixel is equal to 3: the threshold is calculated using the local median in the neighborhood.

 https://doi.org/10.1051/itmconf/20224301014

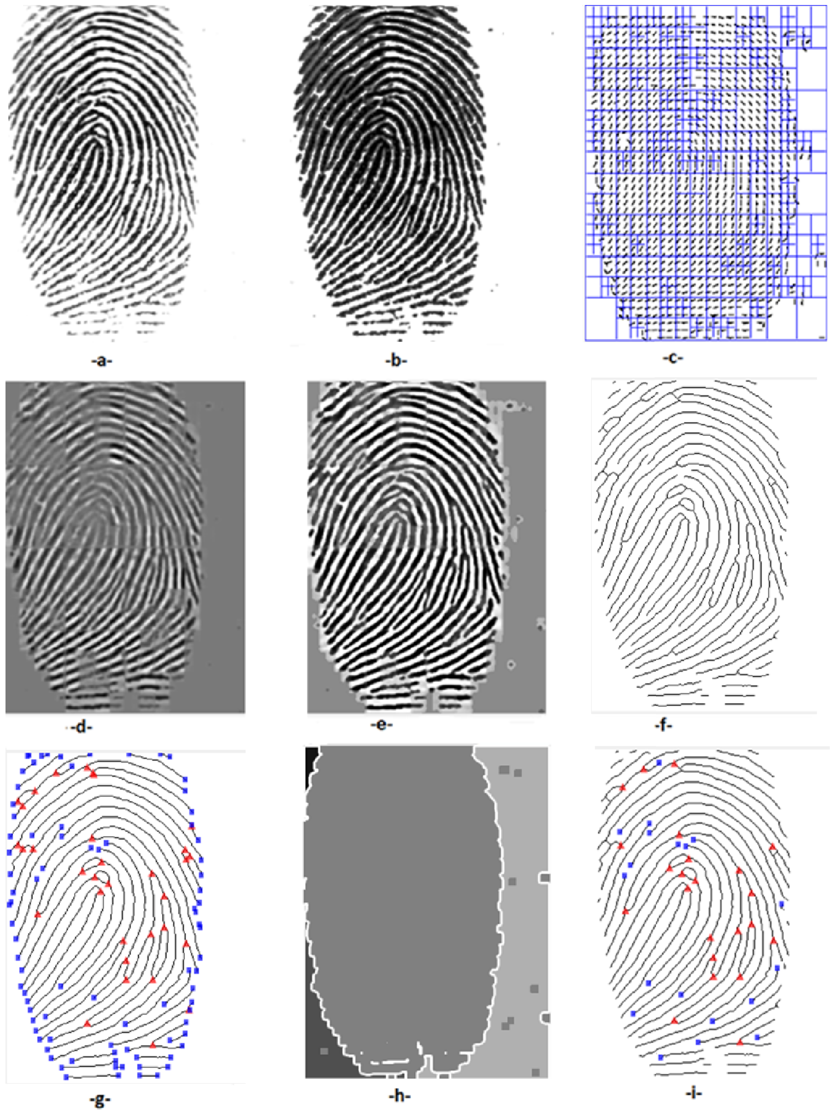

Figure 2: a-Original fingerprint image 103_1 of DB1 FVC2004, -b- Image after histogram equalization, -c- Decomposition of the image according to the orientation field, -d- Output after processing $FFT \times |FFT|^k$ with k=0.45, and applying a gaussian filter for smoothing, -e-Output after Butterworth filtering and binarizing with adaptive thresholding, -f- Thinned fingerprint, -g- Output with detected minutiae, -h- Boundary of the original image, (the process is shown in section 5.1), -i- Detected minutia after post-processing, Number of bifurcation minutia (in **red** triangles): 23. Number of end minutia (in **blue** squares): 19.

Figure 3: a-Original fingerprint image 103_1 of DB1 FVC2004,after histogram equalization, -b- Thinned fingerprint output after processing $FFT \times |FFT|^k$ with k=0.30, -c- with k=0.45, -d- with k=0.55, -e- with k=0.85, -f- with k=1.

6- The final image enhancement step typically performed before extracting minutiae is thinning. Thinning is normally only applied to binary images, and produces another binary image as output. Thinning is a morphological operation that successively erodes away the foreground pixels until they are one pixel wide. This skeleton image is then used in the minutiae extraction [15]. A number of methods have been proposed for correct thinning of a fingerprint image [16]. We use Lam et al. algorithm [12] for thinning the binarized image. Fig. 3 shows the result at the thining phase for a variation of k value for the calculation of the FFT.

7- Minutiae of thinned image are extracted, see section 5. A post-processing is done to remove false minutiae, see section 5.1 and 5.2.

This enhancement process connects broken ridges and removes wrong connections. Figure 2 shows the result of the fingerprint enhancement by our method. The fingerprint image of Figure 2 is of good quality and as expected, the result of our method is as good as that of the reference method [8]. When the quality of the fingerprint image is poor, like in the 103_6 image of DB1 FVC2004 (Figures 10 and 11), our approach gives better results than the reference method [8].

3 Orientation field estimation

W is the neighborhood size used to compute the orientation field image θ. In our approach, W depends on the image quality. The poorer the image quality, the larger W. W values typically varies between 8 and 16. The user specifies quality of the fingerprint image: Bad (W=16), Average (W=12), or Good (W=8). A future work can be the computation of the quality of the fingerprint image.

The ridge orientation field is represented with a matrix or image, θ : in our implementation $\theta(i,j)$ is an orientation angle in $[0,2\pi)$. The orientation $\theta(i,j)$ at pixel (i,j) is computed only for pixels (i,j) such that $W/2 = i \mod W$ and $W/2 = j \mod W$. Such pixels are called θ-pixels. $\theta(i,j)$ depends on $(W+1)^2$ grayscale pixels values $I(i+u, j+v)$ where $u \in [-W/2, W/2]$ and $v \in [-W/2, W/2]$, and I is the fingerprint image after aqualization. $\theta(i,j)$ represents the orientation in the $(W+1)$ by $(W+1)$ square window $(i+[-W/2,W/2], j+[-W/2,W/2])$. A terminal block, *i.e.*, a leave in the quadtree, typically contains many θ-pixels. $\theta(i,j)$ at θ-pixel (i,j) is computed with a gradient-based method [9].

Most of the gradient-based methods [9] rely on the following idea:

1) Calculate the horizontal and vertical Gradients $G_x(i,j)$ and $G_y(i,j)$ image at each pixel $P(i,j)$. Many methods are known: Prewitt, Sobel, Laplacian of Gaussian, Canny, Sobel, Roberts, Fuzzy logic approaches. Sobel filter is sufficient for fingerprint images, and uses convolution: $G_x = M_x \otimes P$, $G_y = M_x^T \otimes P$ [9], where the convolution mask M_x, independent of W, is:

$$M_x = \begin{pmatrix} 1 & 0 & -1 \\ 2 & 0 & -2 \\ 1 & 0 & -1 \end{pmatrix}$$

2) Estimate the local orientation field θ at each θ-pixel (i,j) using the window $(i+[-W/2,W/2], j+[-W/2,W/2])$ using following equations:

$V_x(i,j) = \sum_{u=-W/2}^{W/2} \sum_{v=-W/2}^{W/2} 2G_x(i+u, j+v) G_y(i+u, j+v)$

$V_y(i,j) = \sum_{u=-W/2}^{W/2} \sum_{v=-W/2}^{W/2} (G_x{}^2(i+u, j+v) - G_y{}^2(i+u, j+v))$

$\sigma(i,j) = 1/2 \arctan(V_x(i,j)/V_y(i,j))$
$\theta(i,j) = \sigma(i,j) + k\pi$ where:

$$k = \begin{cases} \frac{1}{2} & \sigma(i,j) < 0 \wedge V_x(i,j) < 0 \\ 1 & \sigma(i,j) < 0 \wedge V_x(i,j) \geq 0 \\ \frac{1}{2} & \sigma(i,j) \geq 0 \wedge V_x(i,j) > 0 \\ 0 & \sigma(i,j) \geq 0 \wedge V_x(i,j) \leq 0 \end{cases}$$

Two orientations θ_1 and θ_2 are close if their angle is smaller than or equal to 10 degrees.

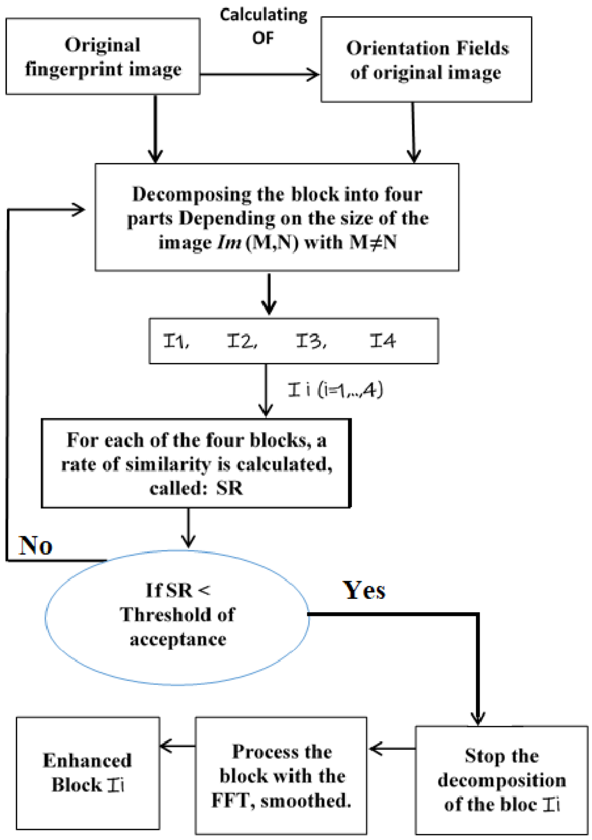

Figure 5: Decision tree of the proposed method of enhancement, the threshold after several tries that we use is 70% of the total number of orientation fields in the block Ii.

4 Decomposition process for enhancement

To compute suitable block size [8], we propose to decompose the orientation field with a quadtree. The flowchart or a decision tree is illustrated in Figure 5. The quadtree permits to recursively subdivide the fingerprint image and its orientation field into homogeneous regions, *i.e.*, regions where the relative similarity rate SR (defined below) is greater than 70%. SR is computed as follows. An example of decomposition is shown in figure 4.

For each θ-pixel (I,J) inside the studied block, compute $B(I,J)$, the set of θ-pixels (i,j) inside the block such that the angle between $\theta(I,J)$ and $\theta(i,j)$ is smaller than 10 degrees.

The absolute similarity rate ASR of the block is the cardinal of its biggest $B(I,J)$ set: ASR=$\max_{I,J} \mid B(I,J) \mid$. The relative similarity rate SR of the block is the ratio of SR

Figure 4: Orientation fields of a fingerprint image (109-5 DB1 FVC2004) after histogram equalization with W=10. -a- orientations in an homogeneous block -b- original image in the block

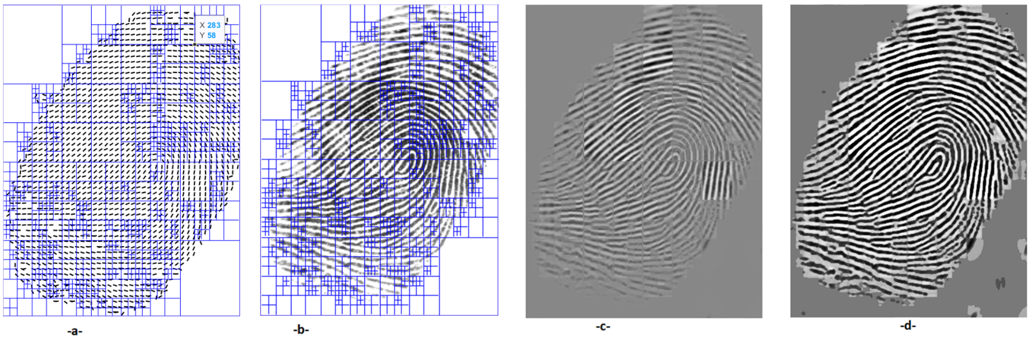

Figure 6: -a- Decomposition of the orientation field into homogeneous blocks -b- superposition with the treated image (107-6 DB1 FVC2004) -c- results after FFT process -d- results after binarization

and of the total number of θ-pixels inside the block. At this stage, ridge pixels are still undetermined. They will be after the binarization step (6).

A block is homogeneous, *i.e.*, it contains close orientations, when its SR is greater or equal to 0.7 (seventy percent). A homogeneous block is suitable for FFT and it is no more subdivided: it gives a leave in the quadtree. When a block is not homogeneous, it is subdivided into four blocks with equal sizes (up to 1 for odd lengths and widths), in order to benefit from the $FFT \times \mid FFT \mid^k$ filter. An example is shown in figure 6.

5 Extracting minutiae and post processing

Once the thinned binary image is calculated, minutiae extraction process is limited to a simple scan of the thinned image to verify the crossing number associated to each ridge pixel (black pixels). The crossing number associated with pixel $P(i,j)$, noted CN(P), is defined by using the eight neighbor pixels as in (2).

$$\mathrm{CN}(P) = 1/2\sum_{i=1}^{8} \mid P_i - P_{i+1} \mid \quad \text{where } P_9 = P_1 \tag{2}$$

P_4	P_3	P_2
P_5	P	P_1
P_6	P_7	P_8

Figure 7: Order of Scan Around pixel P. For convenience, $P_9 = P_1$.

where P_i are the pixel value in the neighborhood of P. See Figure 7. A first post-processing removes border end minutiae and minutiae in missing parts (section 5.1), and a second one removes false bridge minutiae (section 5.2).

A starting or ending minutiae is a black pixel with crossing number 1, and a bifurcation minutiae a black pixel with crossing number 3. Most of black pixels in the thinned image are generic ridges pixels, *i.e.*, their crossing number is 2.

5.1 Removal of border end minutiae and minutia of hidden areas

To remove border minutiae, we apply a morphological closing (or closure) on the complete fingerprint image, and then compute boundaries. That permits to detect fingerprint boundaries, areas with missing parts, and then to remove border minutiae and minutiae inside missing parts. Alter-

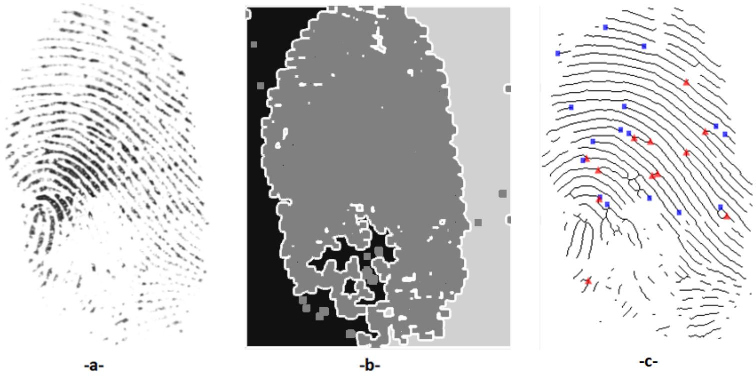

Figure 8: Removing border minutiae and minutia in missing parts.

natively, Shahida Jabeen et al [14], and others, remove border minutiae with the Plus Rule algorithm. But our method eliminates at the same time both border minutiae and minutiae in missing parts. Figure 8 shows the obtained result for image 105_1 in DB1 FVC2004.

5.2 Elimination of false bridge minutiae

False bridge minutiae are false bifurcations generated when two close and parallel ridges are connected, causing a bridge to appear, while there is no real connection between these two ridges. This connection is caused by the poor quality of the digital fingerprint image, and occurs during the binarization stage of the image. To eliminate false bifurcations minutiae of the bridge, the following steps are implemented. For each candidate bifurcation point C of the thinned binary image S (S for skeleton):

1- Clip the thinned binary image with a $W \times W$ window w centered on C.

2- Compute the black connected component of C inside w, using 8-neighborhood and classical Union Find method [17].

3- If a bifurcation of any traversed branch is detected on w boundary, eliminate that bifurcation and the candidate bifurcation C which occurred due to bridge.

Figure 9 shows an example of the process in removal of false bridge minutiae.

6 Implementation, Results and Discussions

Our program is implemented in Matlab (1200 lines), which provides many facilities for image analysis. Treated images are taken from the fingerprint database FVC2004, FVC2002 and NIST Special database SD302-d [20]. They are typically 640×480 size for images of DB1 FVC2004, grayscale (256 levels). Minutiae features of a fingerprint image are extracted in some seconds (less than the time needed for fingerprint acquisition). This treatment is done once and for all for each fingerprint. Minutiae matching methods (and thus their running-time) are not modified by this treatment. When the quality of the fingerprint image is poor, like in the 103_6 image of DB1 FVC2004 (Figure 10, and 11), our approach gives better results than the reference method [8] which uses a fixed initial size block for decomposition. Figures 10 and 11 highlight image parts (surrounded with blue rectangles) where our approach correctly connects broken ridges and where the reference method [8] fails. We observe in Table 1 that with the reference method [8], when the block size for decomposition decreases, the number of false end minutia increases. When the block size increases, the number of false bifurcation minutia increases. That is why our approach is better than the reference method [8]. Table 2 shows the number of Minutiae bifurcations and ridge ends of ten images chosen in DB1-FVC2004, computed with our approach and approach of [8], where the ten images are of poor quality. Table 3 shows a comparison between our approach and Ali et *al*. approach of four images that were chosen by [17] in DB1-FVC2002, who also used FFT for the enhancement stage.

6.1 Standards measurement PSNR and MSE

We use standard measures PSNR and MSE to compare the binary image of the skeleton of the thinned fingerprint of our approach, with the one of the reference method [8]. MSE(X, Y), defined in (3), is the mean squared error between binary images X and Y. MSE is needed to define PSNR (4). PSNR is the peak signal-to-noise ratio between two images. PSNR is often used as a quality measure between an original and a reconstructed image. The higher the PSNR, and the better the reconstructed image. The lower the MSE, the higher the PSNR.

$$MSE(x,y) = \frac{1}{N}\sum_{i=1}^{N}(x_i - y_i)^2 \qquad (3)$$

$$\mathrm{MSE}(X,Y) = \frac{1}{N}\sum_{i}\sum_{j}(X_{i,j} - Y_{i,j})^2 \qquad (4)$$

$$\mathrm{PSNR}(X,Y) = 10\ \log_{10}\frac{L^2}{\mathrm{MSE}(X,Y)} \qquad (5)$$

where N is the total number of pixels in the input image and L is the number of gray levels, here $L = 2$. Table 4 shows PSNR and MSE measures between on one hand the resulting images obtained with our approach, and on second hand the reference method [8] DB1 FVC2004 with block size=4

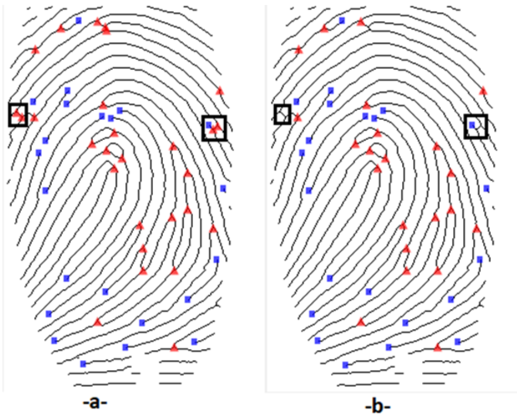

Figure 9: Removing false bridge minutiae on 103_1 image DB1 FVC2004 -a- Number of bifurcation minutia (in **red** triangles): 27. Number of end minutia (in **blue** squares): 22-b- Number of bifurcation minutia (in **red** triangles): 21. Number of end minutia (in **blue** squares): 22.

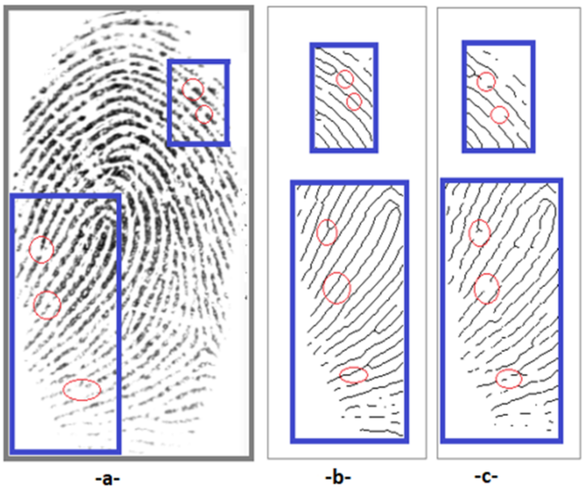

Figure 10: -a-original image -b- thinned part of fingerprint with our approach -c- thinned part of fingerprint with FFT $\times$ $|\mathrm{FFT}|^k$ filter and block size=2.

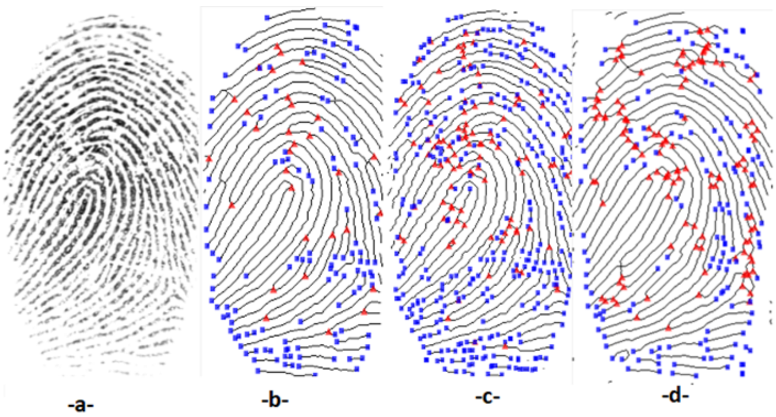

Figure 11: -a- original image 103_6 of DB1 FVC2004, -b- extracted minutia with the proposed approach before post processing, -c- extracted minutia with the reference method [8] and block size=4, -d- extracted minutia with the reference method [8] with block size=16.

(d) and block size=16 (e), for fingerprint image 103_6 used in figure 11. Our PSNR is close to 15.

6.2 Comparison using AER and GI

We tested our approach on DB1 to DB4 database of FVC2004 and on NIST special database SD302d [20]. We choose 100 fingerprints randomly from these datasets.

Table 1: Minutia extraction Comparison of figure 8 with the proposed method and with a fixed block size (image 103_6 of DB1 FVC2004).

Image	Bifurcation	Ridge end
-b- proposed approach	44	84
-c-[8] with block size=4	89	230
-d-[8] with block size=16	105	144

Table 2: Comparison of minutia extraction of 10 fingerprints of FVC 2004images with the proposed method and with a fixed block size (bs)(The ten images are of poor quality).

Image	Approach	Bifurcation	Ridge end
Image1 $DB1 - 103\_7$	proposed approach	49	54
	[8] with bs=4	110	186
	[8] with bs=16	112	71
Image2 $DB1 - 102\_7$	proposed approach	64	72
	[8] with bs=4	107	100
	[8] with bs=16	136	84
Image3 $DB1 - 101\_7$	proposed approach	66	64
	[8] with bs=4	112	93
	[8] with bs=16	116	92
Image4 $DB1 - 104\_2$	proposed approach	71	35
	[8] with bs=4	135	91
	[8] with bs=16	87	66
Image5 $DB1 - 105\_1$	proposed approach	23	29
	[8] with bs=4	100	164
	[8] with bs=16	45	70
Image6 $DB1 - 107\_2$	proposed approach	34	23
	[8] with bs=4	54	172
	[8] with bs=16	54	79
Image7 $DB1 - 107\_7$	proposed approach	62	67
	[8] with bs=4	282	266
	[8] with bs=16	92	133
Image8 $DB1 - 108\_7$	proposed approach	154	85
	[8] with bs=4	322	158
	[8] with bs=16	323	102
Image9 $DB1 - 109\_6$	proposed approach	72	85
	[8] with bs=4	127	158
	[8] with bs=16	128	102
Image10 $DB1 - 110\_6$	proposed approach	97	80
	[8] with bs=4	166	297
	[8] with bs=16	151	188

Table 3: Comparison of minutia extraction of fingerprint image DB1 FVC 2002 with the proposed method and approach of [17].

Images	Minutiae					
	Approach of [17]			Proposed approach		
	Ridge end	Bifurcation	Total	Ridge end	Bifurcation	Total
103_1	41	30	71	24	22	46
101_1	31	11	45	26	15	41
102_1	70	23	93	60	22	82
104_1	59	29	88	58	32	90

We compare minutiae points obtained from the finger- print image using a domain expert of the ground-truth to

Table 4: Performance Metrics PSNR and MSE.

Thinned Image		PSNR	MSE
-b- Our approach	-c- [8] with block size=4	15,14	0.12
	-d- [8] with block size=16	14,87	0.13

minutiae points extracted with our algorithm after post-processing of the same fingerprint image. We define variables P, D, d, e, S, and T: P is the number of paired minutiae points in the fingerprint image, $D = d + e$ the number of missed minutiae points, d the number of dropped, e the number of type exchanged minutiae points, S the number of spurious minutiae points, and T the total number of true minutiae points. We compare the performance of our fingerprint enhancement algorithm with Geevar's [22] and Anandha's [21] by calculating the average error rates (AER) of dropped (d/T), type exchanged (e/T), spurious (S/T) minutiae. Table 5 gives the result of this comparison. We have obtained better results for the average error rates (AER) of dropped minutiae than Geevar [22] and Anandha [21], and better AER for exchanged minutiae than Geevar [22]. Actually, for all possible comparisons, our approach obtains better results.

We also measure the Goodness Index (GI) [18] of our algorithm, from the true minutiae points obtained from the fingerprint image using a domain expert and from the extracted minutiae points after processing our algorithm. The goodness index is defined as:

$$GI = \frac{P - D - S}{T} \tag{6}$$

where $D = d + e$ is the number of dropped and exchanged minutiae. Performance comparison of our method was performed with the standard MINDTCT minutiae extractor established by National Institute of Standards and Technology (NIST) [19]. The GI values in Table 6 were measured, after extracting minutia and post processing with our algorithm, in comparison with minutia provided by MINDCT. The determined GI value of the presented method range from 0.79 to 0.41. The average GI value is 0.61 which is better than Geevar et al. [22] (0.43) who used Short-time Fourier transform (STFT) and similar to Anandha et al. [21] who used the Gabor filter for the enhancement stage.

7 Conclusion

The proposed approach enhances fingerprints relying on orientation fields. The results and the comparison with previous methods [8, 17] show that more broken ridges are connected, and less false minutiae are produced when fingerprint image have a bad quality acquisition. An advantage of our method is the low number of parameters (W, $k = 0.45$, and the homogeneity threshold 70%). Moreover, they have an intuitive meaning. Future work can be the automatic computation of the fingerprint quality image, *i.e.*, the automation of W computation. We can also mention the computation of k value, though $k = 0.45$ (the value we use) works fine, and changing k value has little impact on the quality of the results. Another future work involves Deep Learning with CNN for the enhancement process: the learning set is a set of fingerprint images, and their enhanced fingerprint images, or their corresponding minutiae. Our algorithm, and others, may produce such a learning set.

Table 5: Comparison of average error rate of dropped, spurious and exchanged type minutiae

Method	Dropped (d/T)	Exchanged Type (e/T)	Spurious(S/T)
Proposed	0.0457	0.0698	0.2214
Geevar [22]	0.0967	0.1225	0.1322
Anandha [21]	0.0495	0.0534	0.2215

Table 6: GI value of the proposed algorithm.

Image	T	P	d	e	S	GI
DB1_B_103_1	37	37	0	4	6	0.73
DB1_B_101_2	38	37	1	4	11	0.55
DB2_B_101_1	30	27	3	2	8	0.46
DB2_B_106_3	27	25	2	2	8	0.48
DB3_B_105_2	37	36	1	2	6	0.72
DB3_B_101_3	43	41	2	3	2	0.79
DB4_B_103_5	53	48	5	3	16	0.45
DB4_B_110_3	39	37	2	2	17	0.41
SD302d_2313_M_Pain_01	22	21	1	2	3	0.68
SD302d_2317_M_Plain_02	21	21	0	2	4	0.71

References

[1] Meghna B. Patel, Satyen M. Parikh, Ashok R. Patel Performance Improvement in Preprocessing Phase of Fingerprint Recognition, Information and Communication Technology for Intelligent Systems pp 521-530. 15, December 2018.

[2] Ramesh Chandra Sahoo, Sateesh Kumar Pradhan, A BROAD SURVEY ON FEATURE EXTRACTION METHODS FOR FINGERPRINT IMAGE ANALYSIS, International Journal of Computer Engineering and Technology (IJCET) Volume 10, Issue 2, pp. 14-24, Article ID: IJCET-10-02-002, March-April 2019.

[3] Arucha Rungchokanun, Watcharapong Chaidee, Chonlatid Deerada, Vutipong Areekul, Effect of Pre-Enhancement on False-Rejection Cases of Fingerprint Verification System, 2020 17th International Conference on Electrical Engineering/Electronics, Computer, Telecommunications and Information Technology (ECTI-CON), 04 August 2020.

[4] Anna Czech, Aleksandra Szabelak and Artur Sowinski Changes in Fingerprints Depending on Physiological Factors, PAPER CRIMINALISTICS, Journal of forensic science, Volume 64, issue3, https://doi.org/10.1111/1556-4029.13937, May 2019.

[5] A. K. Jain, L. Hong, S. Pankanti, and R. Bolle,An identity authentication system using fingerprints, IEEE Trans. PAMI, vol. 85, no. 9, pp. 1365-1388, Sept 1997.

[6] Shalash,W.M, Abou-Chadi,F.E.Z.:Fingerprint image enhancement with dynamic block size. In: 23rd IEEE National Radio Science Conference, vol. 0, pp. 1–8, 2006.

[7] A.M. Tahmasebi, S. Kasaei, A novel adaptive approach to fingerprint enhancement filter design, Signal Processing: Image Communication 17, pp. 849-855, 2002.

[8] Neethu S, Sreelakshmi S, Deepa Sankar(2014) 'Enhancement of fingerprint using FFT$\times|$FFT$|^n$ filter', *Procedia Computer Science*, Volume 46, 2015, Pages 1561-1568.

[9] Lukasz WIECLAW, GRADIENT BASED FINGERPRINT ORIENTATION FIELD ESTIMATION, JOURNAL OF MEDICAL INFORMATICS and TECHNOLOGIES Vol. 22/2013, ISSN 1642-6037. 2013.

[10] Chen, Y., Yu, Y.: Thinning approach for noisy digital patterns. Pattern Recogn. (Elsevier) 29(11), 1847–1862 (1996).

[11] Bradley, D., G. Roth, "Adapting Thresholding Using the Integral Image," Journal of Graphics Tools. Vol. 12, No. 2, pp.13–21, 2007.

[12] Lam, L., Seong-Whan Lee, and Ching Y. Suen, "Thinning Methodologies-A Comprehensive Survey," IEEE Transactions on Pattern Analysis and Machine Intelligence, Vol 14, No. 9, September 1992, page 879, bottom of first column through top of second column.

[13] Champod, C., Chamberlain, P.: Fingerprints, Chap. 3. Routledge 2009.

[14] Shahida Jabeen, Shoab Ahmed Khan, "A hybrid false minutiae removal algorithm with boundary elimination",June 2008,DOI: 10.1109/SYSOSE.2008.4724177.

[15] Maltoni, D., Maio, D., Jain, A.K. and Prabhakar S. (2003) Handbook of Fingerprint Recognition, Springer-Verlag.

[16] Neusius, C. and Olszewski J. (1994) 'A noniterative thinning algorithm', ACM Transactions on Mathematical Software, Vol. 20, No. 1, pp.5–20.

[17] Mouad. M.H. Ali ; Vivek H. Mahale ; Pravin Yannawar, "Fingerprint Recognition for Person Identification and Verification Based on Minutiae Matching", 2016 IEEE 6th International Conference on Advanced Computing (IACC). 10.1109/IACC.2016.69. August 2016.

[18] Ratha, N.K., Chen, S., Jain, A.K.: Adaptive flow orientation-based feature extraction in fingerprint images. Pattern Recognition. 28(11), 1657–1672 (1995).

[19] Institute of Standards and Technology, http://www.nist.gov/itl/iad/ig/fpmv.cfm (accessed on: 12/05/2015)

[20] https://www.nist.gov/itl/iad/image-group/nist-special-database-302.

[21] R. Anandha Jothi, J. Nithyapriya, V. Palanisamy, Performance Improvement in Fingerprint Feature Extraction Using Minutiae Local Triangle Feature Set, DOI: 10.1109/IMICPW.2019.8933166, 2019 TEQIP III Sponsored International Conference on Microwave Integrated Circuits, Photonics and Wireless Networks (IMICPW), December 2019.

[22] Greevar et al. "Pre- and Post-fingerprint Skeleton Enhancement for Minutiae Extraction", Proceedings of International Conference on Computer Vision and Image Processing, Advances in Intelligent Systems and Computing 459, 1(2017) 453-465.